Rheol Acta (2002) 41: 532–540
DOI 10.1007/s00397-002-0242-2

ORIGINAL CONTRIBUTION

Maria N. Charalambides
Leonard Wanigasooriya
J. Gordon Williams
Sumana Chakrabarti

Biaxial deformation of dough using the bubble inflation technique. I. Experimental

Received: 2 November 2001
Accepted: 28 January 2002
Published online: 14 May 2002

M.N. Charalambides (✉)
L. Wanigasooriya · J.G. Williams
Mechanical Engineering Department,
Imperial College of Science, Technology
and Medicine, London SW7 2BX, UK
E-mail: m.charalambides@ic.ac.uk

S. Chakrabarti
General Mills, Technology East, 330
University Avenue SE, Minneapolis,
Minnesota 55414-2198, USA

Abstract The bubble inflation test has been used to determine the equi-biaxial stress-strain curve of flour/water dough. This was achieved by undertaking experimental measurements of strain, wall thickness and radius of curvature at the top of the bubble as well as applied pressure. It was observed that the bubble was spherical initially but changed to an elliptical shape at large strains. The analysis derived by Bloksma (1957) was also used to calculate stress and strain at the top of the inflated bubble from gauge pressure and bubble volume data. It was found that the analysis led to accurate bubble heights at moderate strains only, a consequence of the non-spherical bubble shape. In addition, at the top of the bubble, the analytical strain was larger and the thickness was much smaller than the experimental values. The bubble wall thickness distribution was more uniform than the analytical predictions. The discrepancies in bubble height, radius of curvature, strain and thickness had a major effect in the analytical stress-strain curve, as both stress and strain were overestimated, the stress being in error by a factor of four at large strains. Therefore, it is concluded that when the bubble inflation test is used, it is necessary that experimental readings of strain, thickness and radius of curvature as well as pressure should be made to ensure accurate stress-strain curves.

Keywords Dough · Mechanical properties · Stress-strain curve · Bubble inflation

Introduction

It has long been recognised that baking performance and the quality of the finished product, i.e. bread, are strongly dependent on the mechanical properties of the dough used. In addition, knowledge of the material behaviour of dough is a necessary condition for the simulation and optimisation of common processing operations such as mixing, sheeting, extrusion and cutting. As a result of the potential benefits to the food industry, mechanical characterisation of dough has been the subject of several research studies.

As processing operations generally involve large strains, the experimental techniques used need to ensure that the samples are subjected to similar deformations. Large deformation of dough has been studied under lubricated uniaxial compression by Janssen et al. (1996), Bagley and Christianson (1986), Bagley et al. (1988, 1990), Huang and Kokini (1993) and Sliwinski et al. (1996). For an incompressible material tested under frictionless conditions, uniaxial compression is equivalent to equi-biaxial tensile loading. The compression test is by far the most commonly used method as it is very simple to perform. There is no need to grip the sample, which is a problem for a very soft solid such as dough. However, the big disadvantage of the test is the presence of friction between the sample and the loading platens. Such friction leads to a non-homogeneous stress

distribution and invalidates the data. Lubricants can be used to reduce such friction though totally eliminating it is difficult, especially at larger strains. Uniaxial tension tests on dough have been performed by Rasper (1975), Tschoegl et al. (1970) and Meissner and Hostettler (1994). The main problems with this test are the attachment of the dough to the loading grips, the considerable deformation under the weight of the sample and the occurrence of viscous flow of the dough near the clamps.

An alternative to the uniaxial compression and tension tests is the bubble inflation technique. In this test, a sample in the shape of a thin disc is held in a clamp at its circumference and inflated to a spherical 'balloon' using pressurised air (see Fig. 1). In this way, a state of equi-biaxial tension is achieved at the top of the bubble. This method has long been used for the characterisation of synthetic polymers, especially rubbers and polymer melts by many researchers, e.g. Yang and Dealy (1987), Joye et al. (1972), Treloar (1944), Reuge et al. (2001) and Rachik et al. (2001). Apart from dough, other biological materials that have been characterised using the same method include arterial tissue and fruit skins, as reviewed by Shadwick (1992).

The bubble inflation test has been made popular within the dough industry by the belief that it 'simulates' the expansion of the many air cells present in the dough during the baking process (Rasper and Danihelkova 1986). This led to the development of commercial test rigs known as 'alveographs'. Early attempts to derive fundamental properties, i.e. stress-strain relationships, from the alveograph were made by Hlynka and Barth (1955). They assumed that the dough stretches into a bubble which is part of a sphere with a constant wall thickness. This assumption is regarded as a gross approximation as considerable non-uniformity in the thickness of the bubble exists; it is much thinner at the top than at the base of the bubble. Bloksma (1957) derived an analysis that attempts to take into account this non-uniformity in thickness. His analysis has been used in practically all later research without any reservation with the exception of Launay et al. (1977) who performed time-lapse photographic studies to investigate the accuracy in some of the analytical expressions in Bloksma's work. They found that they were accurate only at moderate bubble volumes and air flow rates.

The aim of the current work is to use the bubble inflation technique in order to determine the stress-strain relationship of dough under equi-biaxial loading conditions. Specifically, the accuracy of the analysis proposed by Bloksma will be investigated by comparing with independent experimental measurements of bubble height, strain and thickness.

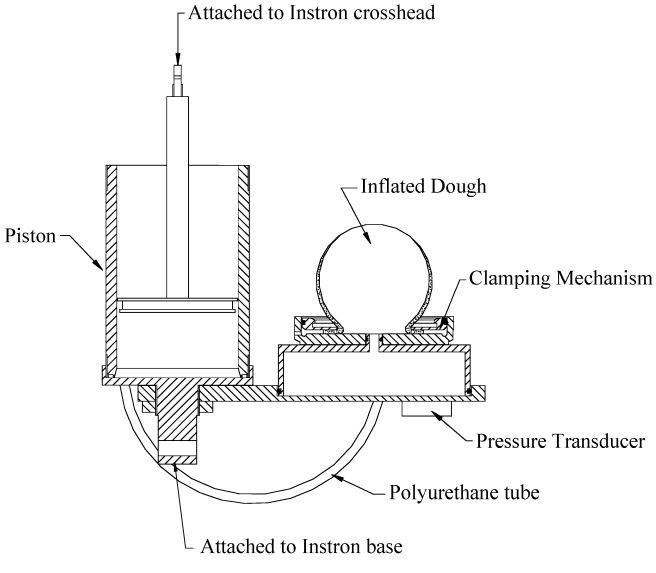

Fig. 1. Schematic of bubble inflation test rig

Experimental procedures

Simple flour/water dough was mixed using a laboratory six-pin mixer capable of recording torque during the mixing process. The flour was supplied by General Mills (USA) with a blend composition of: 13.25% ± 0.75% moisture, 10.5% ± 0.35% protein and 0.5% ± 0.03% ash contents. Ash and protein are both quoted on the 14% moisture basis standard. The dough was made by mixing 198.5 g of flour with 120 g distilled water and 1.5 g salt (sodium chloride), giving a total of 320 g of dough from each mix. The flour and salt solution were pre-chilled to –20 °C and 3 °C respectively. The speed of the mixer was kept constant at 118 rpm. The mixing duration was kept constant at 3 min for all samples. The final dough temperature was in the range of 17–19 °C.

Similar sample preparation procedures to those described by Dobraszczyk (1997) and Dobraszczyk and Roberts (1994) were followed. The mixed dough was rolled into a sheet, approximately 6 mm in thickness. Circular disks were then cut out using a 50 mm diameter pastry cutter. Each disk was placed into a specially made clamping device and flattened with a manual press to form a sample with a thickness of 1.5 mm and a diameter of 55 mm. After the samples were prepared they were left at room temperature for a minimum of 45 min before testing. A thin coating of paraffin oil was applied on the exposed surfaces to prevent drying of the samples.

The bubble inflation rig was manufactured at Imperial College, based on the design by Dobraszczyk and Roberts (1994). It was built such that it could be mounted on a conventional Instron testing machine. The piston is attached on the crosshead of the machine. When the crosshead is displaced downwards, the air trapped in the system is displaced, thus inflating the dough sample (see Fig. 1). The crosshead speed was kept constant at 50 mm/min for all tests. The cross sectional area of the piston was 7.9×10^{-3} m^2. All samples were tested at room temperature that was kept constant at 21 °C. The radius of the samples was 27.5 mm.

The pressure inside the dough bubble was continuously monitored via a 50-mbar pressure transducer (HCXM050D6V Farnell), which was calibrated prior to the tests using an airline and a manometer. An A-D converter was used to input the transducer signal vs time to a computer. The displacement of the piston is recorded directly by the Instron so that gauge pressure-piston displacement data are obtained.

The height of the bubble was measured using a Hitachi Denshi CCD camera positioned such that the side of the bubble was in view. The CCD images were analysed using image analysis software (NIH-image). The same images were used to determine the shape of the bubble, by measuring the major and minor axis, α and β respectively (see Fig. 2). Such measurements were only possible once the bubble height exceeded its radius. For a perfectly spherical shape α and β should be equal. Note that for abbreviation purposes the bubble is called spherical even though it is only a part of a sphere as the lower portion is not present, i.e. where the clamp holds the bubble.

The strain at the top of the bubble was measured by positioning the camera directly above the bubble. The strain during inflation was based on analysing the deformation of an orthogonal grid painted on to the sample before inflation (see Fig. 3). Food colouring (Supercook black) and a circular brass plate with vertical lines of 0.3 mm width and a distance of 1.7 mm between each line were used to produce the grid. The paint was air brushed on to the stencil giving 28 lines in one direction. By rotating the stencil 90°, lines in the orthogonal direction were obtained to form a grid. For effective lighting, fibre optical lights were used. The distance between the camera lens and the top of the bubble was continuously changing during inflation, thus causing a change in the magnification factor. This was taken into account in the analysis by incorporating a calibration factor. The effect of the bubble curvature on the measured grid deformation and hence the strain was also investigated and it was found to be negligible. Images showing the deformation of the grid at various strains are shown in Fig. 3.

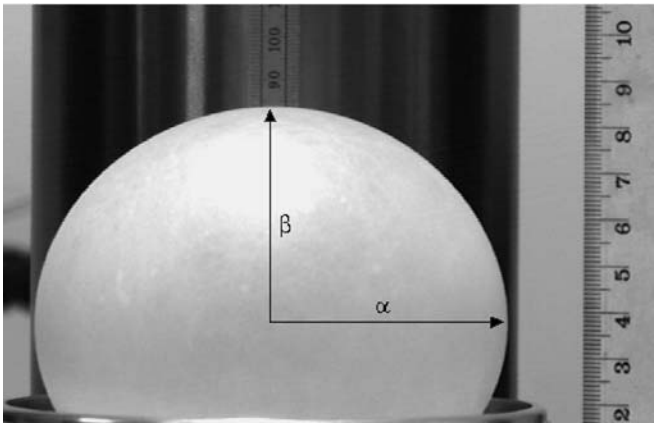

Fig. 2. Side view of the inflated sample

In order to measure the thickness of the bubble, the inflation process was interrupted by stopping the crosshead movement when the samples reached various heights smaller than the failure height. The bubble was then allowed to dry at room temperature. Once the bubble top was dry, a section was cut out and the thickness measured using a digital micrometer. The amount of time needed to dry the sample fully was impractically large at bubble heights less than 35 mm; hence no data were obtained in that region.

The bubble height was measured at the beginning and end of the drying process and the disagreement was only 0.3%. In addition, the grid on the samples was used to check the effect of drying on strain, by comparing the strain when the inflation was stopped, to the strain just before the dried sample was cut. A disagreement of approximately 7% was observed. This was probably due to the shrinkage of the sample during drying. Note that the reduction in weight of the dough due to drying was experimentally found to be around 30%. As density of dough and water are very close, the reduction in volume due to drying is also expected to be around 30%. This implies approximately a 10% decrease in each of the three dimensions. Therefore, there is confidence that the dried bubble thickness is a good approximation to the actual non-dried bubble thickness.

One sample inflated to a height of 81 mm was left to dry for sufficient time such that the sides as well as the top of the bubble were dry. This allowed the thickness distribution along the bubble to be determined.

An alternative method of measuring the bubble thickness was investigated. Samples were inflated to various heights and the top of the bubble was frozen using liquid nitrogen. The frozen section was cut and then measured with a digital micrometer. The micrometer anvils were frozen to reduce the heat transfer between the anvils and the element. It was observed that a sheet of ice was formed on all the samples, leading to thickness measurements that were erroneously high so the method was not investigated further.

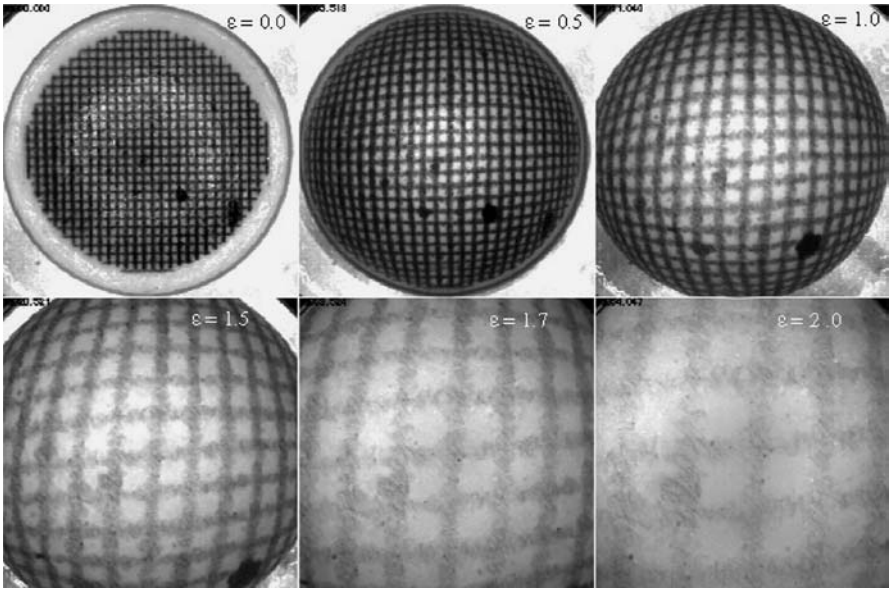

Fig. 3. Deformation of orthogonal grid at various strains

Analysis

As mentioned earlier, Bloksma (1957) proposed an analytical procedure for calculating the stress and strain at the top of the bubble from the experimental data. The analysis is based on the following assumptions: i) the dough is incompressible, ii) the bubble is spherical and iii) each dough particle is shifted normally to itself during inflation.

As the bubble inflates, the wall thickness reduces. However, due to the non-uniform deformation along the surface of the bubble, the thickness at the top is smaller than the thickness at the base of the bubble close to the clamp and a thickness distribution arises. Bloksma (1957) derived the following relationship describing this distribution:

$$t = t_0\left[\frac{a^4 + s^2h^2}{a^2(a^2+h^2)}\right]^2 \tag{1}$$

where t_0 is the original sample thickness, a the original sample radius, h the bubble height and t the thickness of the small element whose original position is described by the distance s from the centre of the sample (see Fig. 4). Note that the path of the element shown in Fig. 4 by two arcs, is determined by the third assumption stated above, i.e. that each element is shifted normally to itself during inflation. The thickness at the top of the bubble, t_t, is then derived by setting $s=0$ in Eq. (1):

$$t_t = t_0\left(1+\frac{h^2}{a^2}\right)^{-2} \tag{2}$$

The height of the bubble can be calculated by considering the volume, V, of the air enclosed in the bubble:

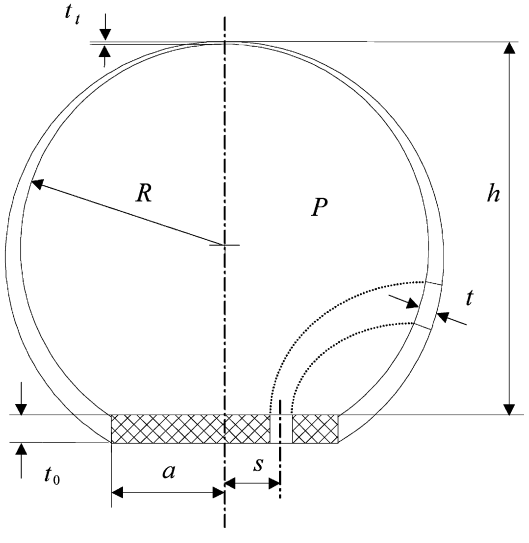

Fig. 4. Geometry of bubble expansion

$$V = \frac{\pi}{6}h\left(3a^2+h^2\right) \tag{3}$$

This volume can be calculated via two methods:

1. Assume that the pressure, P, is so small that V is equal to the volume of air displaced by the piston, i.e. incompressible behaviour of the air.
2. Use perfect gas law at constant temperature (PV=constant) to derive the new volume of the displaced air enclosed in the system and hence in the bubble.

Both assumptions were investigated and it was found that there was negligible effect on the results. Thus, assumption 1, which involved the simplest calculation, will be used throughout. In that case V is given by

$$V = A\delta \tag{4}$$

where A is the cross sectional area of the piston (7.9×10^{-3} m^2) and δ is the piston displacement. Equation (3) is solved for h using the Newton-Raphson numerical method.

Considering the geometry of the bubble, the radius R is given by

$$R = \frac{a^2+h^2}{2h} \tag{5}$$

Using the incompressibility assumption together with Eq. (2), the planar strains ϵ_x, ϵ_y and the strain through the thickness, ϵ_z, at the top of the bubble are given by

$$\varepsilon_x = \varepsilon_y = -\frac{1}{2}\varepsilon_z = \ln\left(1+\frac{h^2}{a^2}\right) \tag{6}$$

Finally, the stress, σ, is calculated from the usual relationship for a pressurised spherical vessel:

$$\sigma = \frac{PR}{2t_t} \tag{7}$$

where P is the pressure inside the bubble. Note that the same relationships for t, σ and ϵ_x can be derived from large strain theory of membranes (Williams 1980).

An alternative analysis can be performed if the assumption of a uniform bubble thickness is made. Again assuming incompressibility, the thickness can be calculated from

$$t = \frac{\pi a^2 t_0}{S} \tag{8}$$

where S is the corresponding surface area of the bubble. The latter is given by

$$S = 2\pi R^2 \pm 2\pi R\sqrt{R^2-a^2} \tag{9}$$

where the positive and negative signs are for the cases of $h > R$ and $h < R$ respectively. Note that at $h = R$, $R = a$ and the two solutions result in the same answer.

Results

The experimentally measured bubble height and that calculated using Eqs. (3) and (4) are compared in Fig. 5. It is apparent that for heights less than 60 mm the experimental and analytical values are in good agreement. For larger heights, a deviation is observed reaching a maximum of approximately 9% at heights equal to 80 mm. This implies that the assumption of a perfect spherical shape is only accurate at moderate strains. This conclusion is further supported by the results shown in Fig. 6, where measurements of the major and minor axes α and β respectively from two replicate tests are plotted. It is observed that for α larger than 35 mm, which corresponds to h larger than 58 mm, α is noticeably larger than β. This deviation from a perfect spherical shape was evident during the tests as at large strains the bubble assumed a slight elliptical shape with a 'flattened' top (see Fig. 2). The ratio α/β will be referred to as k. From Fig. 6, k is 1.1 for h larger than 58 mm whereas for h smaller than 58 mm, k is equal to 1.0.

Figure 7 shows the average pressure vs bubble height data. The curve shown is the average from all 23 tested samples. The usual peak is observed which has no significance in terms of the stress-strain curve as the latter shows no maximum or inflection points coinciding with the peak in the pressure plot (see Fig. 12).

The results from the tests where the strain was measured directly by analysing the deformation of the painted grid are shown in Figs. 8 and 9. The assumption regarding the equi-biaxial deformation at the top of the bubble is justified by the results of Fig. 8, where the strains in the two planar directions, ϵ_x and ϵ_y, are shown to be almost equal to each other. The measured strain is

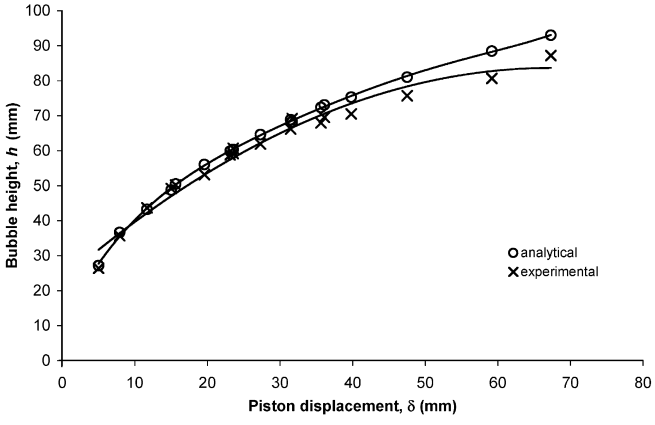

Fig. 5. Comparison of experimental and analytical bubble height

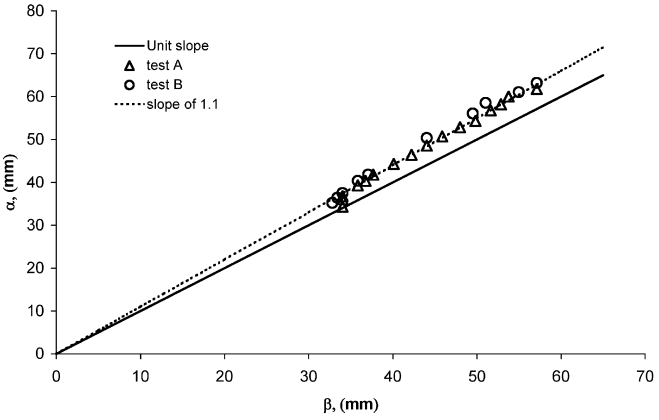

Fig. 6. Accuracy of spherical shape assumption

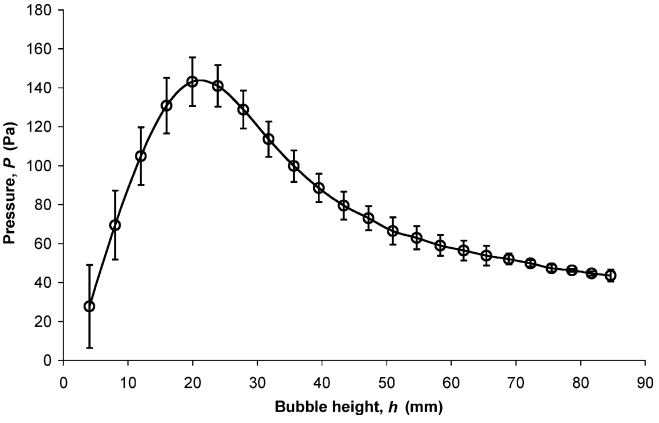

Fig. 7. Pressure vs bubble height

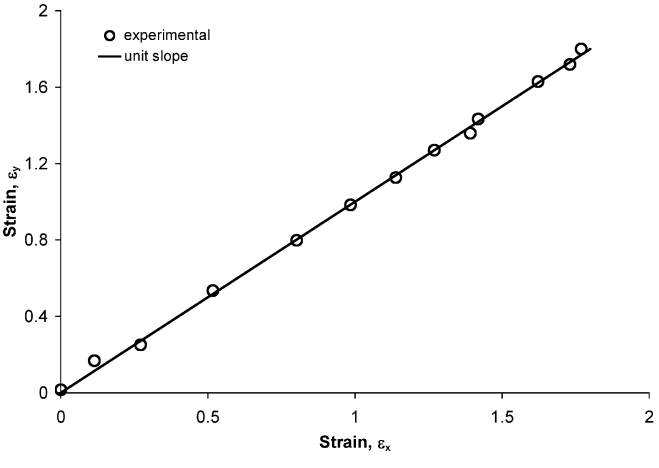

Fig. 8. Evidence of equi-biaxial loading conditions at the top of the bubble

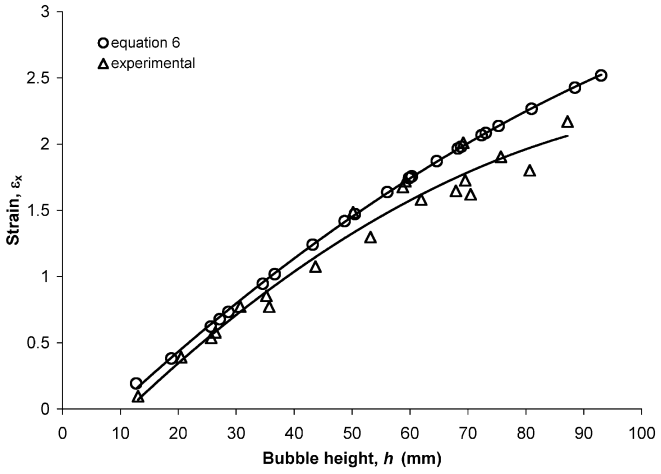

Fig. 9. Strain at the top of the bubble vs bubble height

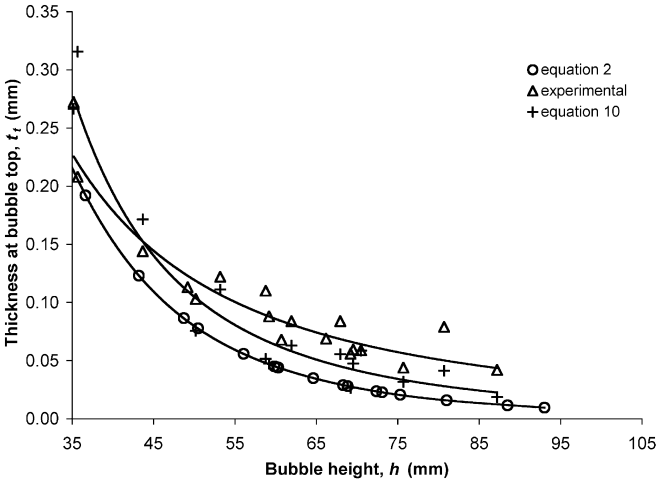

Fig. 10. Thickness at the top of the bubble vs bubble height

compared with the analytical strain (Eq. 6) in Fig. 9. Each point in Fig. 9 corresponds to a single test where the inflation was stopped at various bubble heights such that the bubble thickness could be measured as well. Considerable scatter is observed highlighting the variability of dough as well as the complexity of the measurements. Nevertheless, it is apparent that the analytical strains are larger than the experimental ones.

The thickness at the top of the bubble was also investigated. Analytical values were calculated from Eq. (2) and experimental values were obtained from the dried samples. In addition, the following relationship can be derived from Eq. (6):

$$t_t = t_0 e^{-2\varepsilon_x} \tag{10}$$

so that an extra set of thickness data can be derived by substituting the experimentally measured strains in Eq. (10).

The three sets of data are plotted vs bubble height in Fig. 10. It is apparent that the thickness calculated from Eq. (2) is the smallest and that the one physically measured after the bubble had dried is the largest of the three. The fact that Eqs. (6) and (10) would lead to an underestimation of the thickness is anticipated, as it was shown earlier in Fig. 9 that the actual strain ϵ_x at the top of the bubble is smaller than the analytical value. This of course implies that the actual strain ϵ_z is also smaller than predicted.

Experimental data for the bubble thickness as a function of the distance s are compared with analytical data (Eq. 1) in Fig. 11. It is observed that the predictions are far from the experimental values. The real distribution of thickness and hence strain along the bubble is more uniform than the analytical one. As a result, the thickness at the top of the bubble is much larger than the analytical predictions. The disagreement between the two decreases for increasing s up to

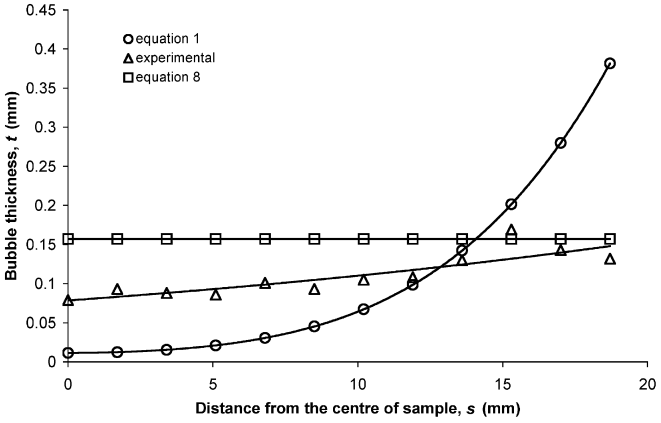

Fig. 11. Distribution of bubble wall thickness

$s = 12.8$ mm and thereafter the predicted value overestimates the measured one.

As the thickness distribution was more uniform than Bloksma's analysis predicted, it was decided to investigate the accuracy of the alternative assumption of uniform thickness. Equations (8) and (9) are used to calculate the new thickness and the result is displayed in Fig. 11. However, once again there is no agreement with the measured value. At the top of the bubble, the thickness is now overestimated by a factor of two. As the prediction is rather poor, no further analysis was conducted with the constant thickness assumption.

The elliptical shape of the bubble at larger strains means that the radius R as calculated by Eq. (5) will be in error. The correct radius of curvature at the top of the bubble, R_c, can be calculated by

$$R_c = \frac{[1 + f'x(0)]^{\frac{3}{2}}}{f''x(0)} \tag{11}$$

where $f'x(0)$ and $f''x(0)$ are the first and second derivatives respectively of the function $f(x)$ describing the shape of the bubble, evaluated at $x=0$. As the shape is elliptical (see Fig. 2), $f(x)$ is

$$f(x) = \beta\left(1 - \frac{x^2}{\alpha^2}\right)^{\frac{1}{2}} \tag{12}$$

The height of the bubble h can be written as

$$h = \beta + f(a) \tag{13}$$

Equations (11), (12) and (13) lead to

$$R_c = \frac{a^2 + k^2h^2}{2h} \tag{14}$$

where k is the ratio α/β. Note that for $k=1$, the bubble is spherical and Eq. (5) is recovered.

Therefore, this corrected value for the radius of curvature at the top of the bubble should be used in Eq. (7) instead of R. From the experimental observations presented above the value of k should be equal to 1.0 for $h < 58$ mm and equal to 1.1 for $h > 58$ mm. This will lead to the correct value for σ, provided P and t_t are also accurate.

Finally, the stress-strain curve is investigated. One experimental and one analytical point was derived from each test such that corresponding stress-strain curves were obtained. The true, 'experimental' curve is shown in Fig. 12. This is the true curve as the strain was determined experimentally and the stress was calculated from Eq. (7) using the experimental values of P, t_t and R_c. Note that the latter requires the values of h and k which were also determined experimentally.

The 'analytical' curve is also shown in Fig. 12 for comparison purposes. In this case the strain was calculated from Eq. (6). Both R and t_t needed in Eq. (7) for the calculation of σ, were calculated using Eqs. (5) and (2) respectively. Therefore, in this case, the only experimental measurements that are needed are the pressure, P and the piston displacement, i.e. the bubble volume, V.

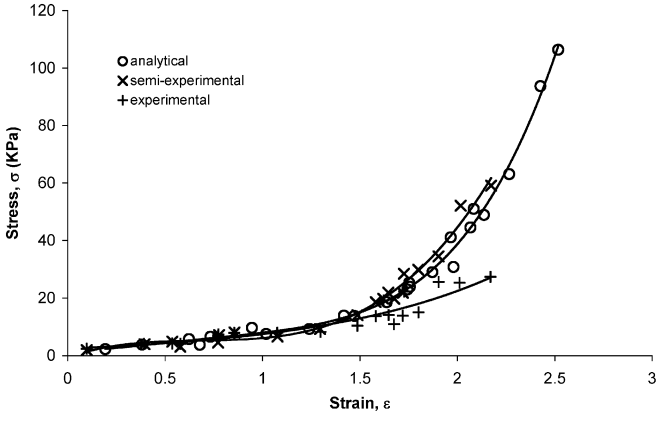

Fig. 12. Stress-strain curves

From Fig. 12, it is observed that the analytical curve is in error. The stress is overestimated by a factor of four at large strains. The strain is also overestimated but by a much smaller amount (see Fig. 9). This disagreement between the analytical and the experimental curve points to the inaccuracy of the simplifying assumptions in Blokma's analysis regarding the shape of the bubble, the material's incompressibility and the wall thickness distribution.

Figure 12 shows an additional curve called 'semi-experimental'. This curve was determined in an identical way as the experimental curve apart from the thickness, t_t, which was calculated using Eq. (10), i.e. assuming the dough is incompressible. This was used in Eq. (7) to calculate the stress. Therefore the experimental measurements that are needed in this case are ϵ, P and R_c (hence h and k). The importance of this case lies in the fact that there is no need to interrupt the tests at various heights to allow the bubble to dry. This would lead to less experimental scatter and hence a smaller number of tests as each experiment would lead to a continuous trace of the stress-strain curve. In addition to the practical implications, this case also allows the accuracy of the incompressibility assumption to be determined, as the latter is the only assumption that is made in this case.

From Fig. 12, it is apparent that the stress at large strains in the 'semi-experimental' curve is still overestimated, this time by a factor of two. Therefore, it is concluded that the compressibility of the dough of this study cannot be ignored as it has a large effect on the calculated stress values. Also of interest is the fact that the semi-experimental and analytical curves are very close to each other. This has no significance however as the same instant during the inflation process corresponds to a different stress-strain point along the same curve.

In order to bring the semi-experimental data closer to the experimental data, the assumption of incompressibility needs to be relaxed. Incompressibility implies that the Poisson's ratio, v, is equal to 0.5. Hooke's law applied to bi-axial loading leads to the following relationship between the strains ϵ_x and ϵ_z:

$$\varepsilon_z = -\frac{2v}{1-v}\varepsilon_x \tag{15}$$

For a value of v equal to 0.46, Eq. (15) becomes

$$\varepsilon_z = -1.704\varepsilon_x \tag{16}$$

Therefore the thickness at the top of the bubble can be calculated from

$$t_t = t_0 e^{-1.704\varepsilon_x} \tag{17}$$

Note that the coefficient of ϵ_x now becomes –1.704 compared to –2 in Eq. (10). Using these new values of t_t

in the calculation of stress leads to the stress-strain curve shown in Fig. 13 (semi-experimental, $v = 0.46$). The original curve (semi-experimental, $v = 0.5$) as well as the experimental data are re-plotted for comparison purposes. It is observed that changing v from 0.5 to 0.46 shifts the data downwards by approximately 100% at large strains, bringing them very close to the experimental data. Therefore, if v is known a priori, the independent measurement of bubble wall thickness is not necessary.

Finally, the experimental strain data can be used to determine the strain rate during the test as shown in Fig. 14. The results are not very accurate as they are obtained from differentiation of experimental data that were smoothed. Nevertheless, it is obvious that a large variation in strain rate is occurring with a substantial decrease in the strain rate as the test progresses. This variation is a consequence of the constant inflation rate, i.e. constant crosshead speed during the test. This complicates the analysis of the test even more as the strain rate needs to be constant for a highly viscoelastic material such as dough. Therefore, efforts should be made to perform the tests under constant strain rate by using a testing machine that is capable of adjusting the crosshead speed according to changes in the strain, via a feedback loop control system.

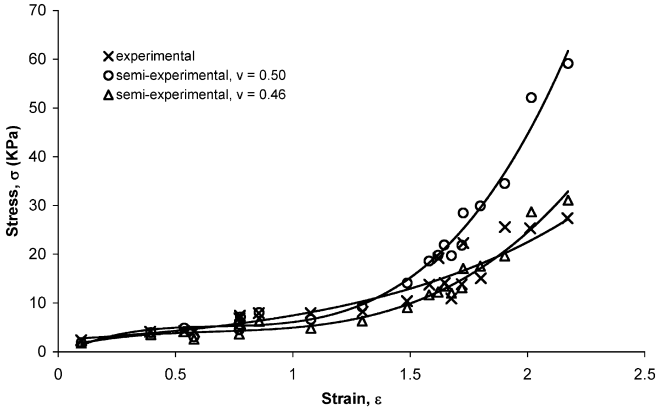

Fig. 13. Effect of Poisson's ratio on semi-experimental stress-strain curves

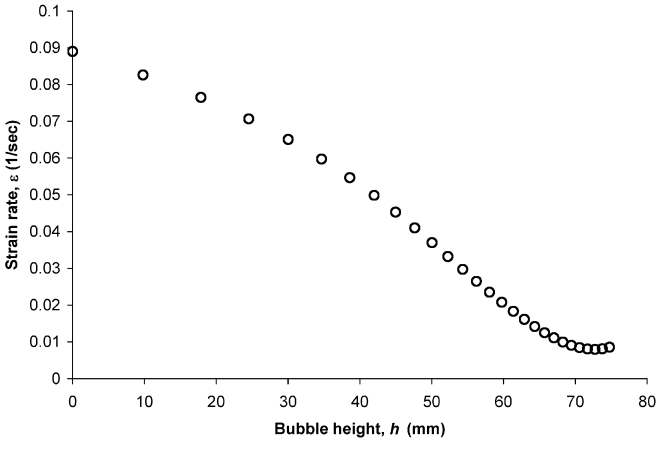

Fig. 14. Strain rate variation

Conclusions

The correct stress-strain curve of the dough under investigation has been determined. This was achieved by undertaking experimental measurements of strain, wall thickness and radius of curvature at the top of the bubble as well as applied pressure.

These measurements are quite complicated and thus prone to experimental scatter as well as being time-consuming. A much simpler way would be to derive the stress-strain curve with the aid of an analytical procedure that can be used to predict test variables such as strain, wall thickness and radius of curvature. Such an analysis was derived by Bloksma (1957) and has been used in several dough studies. However, it has been shown that for the material and test conditions of this study, Bloksma's analysis leads to serious errors in the calculated stress-strain curve, with the stress overestimated by a factor of four at large strains. This is due to the invalid simplifying assumptions in the analysis.

The first assumption in the analysis regarding the spherical shape has been shown to be accurate at moderate strains only. At larger strains, the bubble assumed an elliptical shape with a ratio of major to minor axis equal to 1.1.

The assumption regarding the incompressibility of the material was also found to be inaccurate. The compressibility could be due to the air pockets introduced in the dough during mixing. When a Poisson's ratio of 0.46 is used instead of 0.5, the semi-experimental data become very close to the experimental data.

The strain at the top of the bubble was also overestimated by Bloksma's analysis although by a much smaller amount than the overestimation in stress. In addition, the analytical wall thickness distribution was not realistic. The experimental thickness distribution was far more uniform than the analytical value. The experimental values for the thickness at the top of the bubble were much larger than the analytical values.

It is not known how a different dough composition and/or different inflation rate and temperature would affect the accuracy of the analytical assumptions. Launay et al. (1977), who also investigated the analytical thickness distribution, stated that its accuracy decreased with increasing inflation rate and bubble height. A study is presently underway whose aim is to examine the effect of the inflation rate on the accuracy of the analytical derivations.

The implication of the large error in the stress-strain curve is that bubble inflation tests should only be undertaken if experimental readings of strain, thickness and radius of curvature as well as pressure are recorded. This makes the test far less attractive as these measurements are complex and time-consuming. Ideally, an alternative method for measuring the thickness at the top of the bubble should be used, which will allow continuous recording of the thickness. The use of lasers is currently being investigated. As the errors are so large, it is believed that a finite element numerical analysis of the bubble inflation test should be performed. This would enable comparisons to be made between analytical, experimental as well as numerical data and would aid in the deeper understanding of the problem.

Acknowledgements The authors would like to acknowledge the financial support of General Mills, USA. They would also like to thank Dr B. Dobraszczyk of University of Reading for the advice regarding many aspects of the bubble inflation test and Mr A. Oppenheimer of General Mills for his advice on dough preparations.

References

Bagley EB, Christianson D (1986) Response of chemically leavened doughs to uniaxial compression. In: Faridi H, Faubion JM (eds) Fundamentals of dough rheology. Americal Association of Cereal Chemists, St Paul, MN, 27–36

Bagley EB, Christianson DD, Martindale JA (1988) Uniaxial compression of a hard wheat flour dough. J Texture Stud 19:289–305

Bagley EB, Christianson DD, Trebacz DL (1990) The computation of viscosity and relaxation time of doughs from biaxial extension data. J Texture Stud 21:339–354

Bloksma AH (1957) A calculation of the shape of the alveograms of some rheological model substances. Cereal Chem 34:126–136

Dobraszczyk BJ (1997) Development of a new dough inflation system to evaluate doughs. J Am Assoc Cereal Chem 42:516–519

Dobraszczyk BJ, Roberts CA (1994) Strain hardening and dough gas cell-wall failure in biaxial extension. J Cereal Sci 20:265–274

Hlynka I, Barth FW (1955) Chopin alveograph studies. I. Dough resistance at constant sample deformation. Cereal Chem 32:463–471

Huang H, Kokini JL (1993) Measurement of biaxial extensional viscosity of wheat flour doughs. J Rheol 37:879–891

Janssen AM, van Vliet T, Vereijken JM (1996) Rheological behaviour of wheat glutens at small and large deformations. J Cereal Sci 23:19–31

Joye DD, Poehlein GW, Denson CD (1972) A bubble inflation technique for the measurement of viscoelastic properties in equal biaxial extensional flow. Trans Soc Rheol 16:421–445

Launay B, Bure J, Praden J (1977) Use of the Chopin Alveographe as a rheological tool. I. Dough deformation measurements. Cereal Chem 54:1042–1048

Meissner J, Hostettler J (1994) A new elongational rheometer for polymer melts and other highly viscoelastic liquids. Rheol Acta 33:1–21

Rachik M, Schmidt F, Reuge N, Le Maoult Y, Abbe F (2001) Elastomer biaxial characterisation using bubble inflation technique. I. Experimental investigations. Polym Eng Sci 41:532–541

Rasper VF (1975) Dough rheology at large deformations in simple tensile mode. Cereal Chem 52:24–41

Rasper VF, Danihelkova H (1986) Alveography in fundamental dough rheology. In: Faridi H, Faubion JM (eds) Fundamentals of dough rheology. American Association of Cereal Chemists, St Paul, MN, pp 169–180

Reuge N, Schmidt FM, Le Maoult Y, Rachik M, Abbe F (2001) Elastomer biaxial characterisation using bubble inflation technique. I. Experimental investigations. Polym Eng Sci 41:522–531

Shadwick RE (1992) Soft composites. In: Vincent JFV (ed) Biomechanics-materials, a practical approach. IRL Oxford University Press, pp 133–163

Sliwinski E, van Vliet T, Kolster P (1996) On the relationship between large deformation properties and biochemical parameters of wheat flour dough in relation to breadmaking quality. In: Proceedings of 6th International Gluten Workshop, North Melbourne, Australia, pp 211–217

Treloar LRG (1944) Strains in an inflated rubber sheet and the mechanism of bursting. Trans Inst Rubber Ind 19:201–212

Tschoegl NW, Rinde JA, Smith TL (1970) Method for determining the large deformation and rupture properties in simple tension. J Sci Food Agric 21:65–70

Williams JG (1980) Stress analysis for polymers. Ellis Horwood, Chichester, pp 231–245.

Yang MC, Dealy JM (1987) Control of strain rate in a sheet-inflation rheometer. J Rheol 31:113–120